Post compression of high-energy femtosecond laser pulses using bulk media

Master Thesis
by
Elisabeth Wieslander

Lund Reports on Atomic Physics, LRAP-293
Lund, January 2003

Abstract

In this Master Thesis the first step towards post pulse compression of femtosecond pulses using bulk media is implemented at the Terawatt laser facility CELIA in Bordeaux. A reflection of the terawatt laser's main beam is used, with pulse energies of 450 μJ and 30 fs pulse duration. After the bulk, a prism compressor is used to compress the pulses and the pulse duration is measured with a multishot autocorrelator. The combined effect of *self phase modulation* and *group velocity dispersion* that the pulse experiences in the bulk material, BK-7, result after compression in pulses as short as 10 fs and with an energy of 50 μJ.

Contents

1 Introduction

1.1 Short pulses

Ever since the laser was invented in 1960 the scientific community has tried to decrease the duration of the laser pulses, as shown in Figure 1 below. Short pulses are interesting for studying ultrashort processes, e.g. ultra fast chemical reactions. The pulses are also used in applications requiring high peak power, since the peak power is proportional to the inverse of the pulse duration. Laser pulses with durations less than 0,1 ps are often called *ultrashort pulses* and their behaviour is discussed in further detail in this Master Thesis.

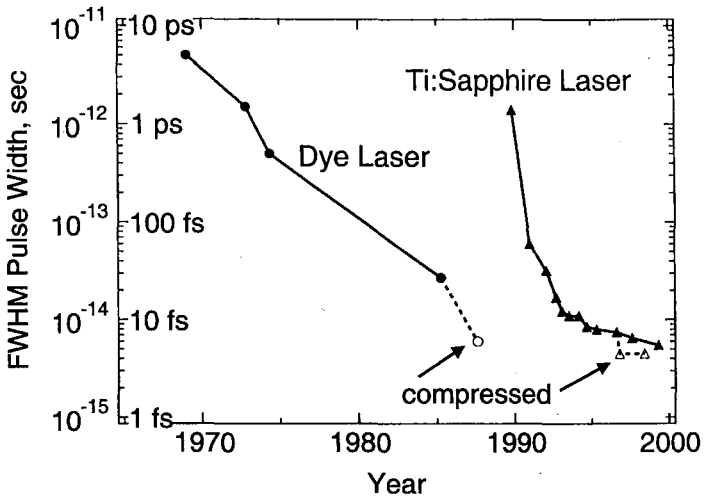

Figure 1. *The pulse duration as a function of the past years.*

Shorter duration of the ultrashort pulses can be done in two ways:

- Improvements of the laser cavity
- Post compression of the laser pulses

A combination of these two ways has shortened the pulse duration quite rapidly over the past years. Changes of the laser cavity include Q-switching, cavity dumping and mode locking. In 1984 it was shown that fibers and optical gratings can be used to compress laser pulses and the most common ways to achieve post compression are:

- Pulse compression through a hollow wave-guide while the wave-guide is filled with noble gases at a variable pressure. This method produces the shortest pulses today. However, the drawback is that fibers are limited to relatively low energy due to material damage and non-linear effects occurring at too high input energies.

- Pulse compression using a glass material (bulk). The advantage is that the medium can withstand higher pulse energies than the fiber. This high-power broadening can be obtained in almost any frequency region by using the appropriate material. The conditions for broadening and compression are different depending on the material.

1.2 The principles of post compression in bulk material

The pulse duration and bandwidth of a laser pulse are related by the *time-bandwidth uncertainty*:

(1) $\Delta\omega \cdot \Delta\tau \geq const$

where $\Delta\omega$ is the frequency bandwidth and $\Delta\tau$ is the pulse duration. Equation (1) states that the product of time and bandwidth is greater or equal to a constant, which implies that if you increase the bandwidth then you might decrease the time duration.

To increase the bandwidth, the fact that most transparent materials have an intensity dependent refractive index is used. When the laser pulse travels through the transparent media the different parts of the pulse experience different refractive indices resulting in *spectral broadening*. If the pulse is approximated to be Gaussian, as in Figure 2, it is easy to understand that the pulse will be broadened due to the time dependence of the intensity envelope and this effect is called the *optical Kerr effect.*

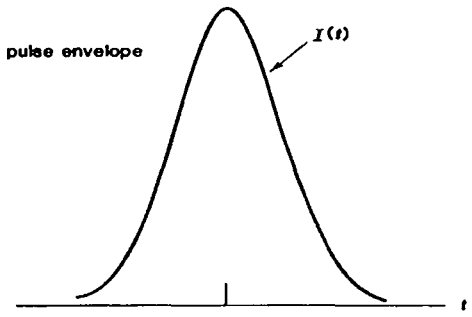

Figure 2. *The shape of a Gaussian pulse.*

An expression for the refraction index is then

(2) $n = n_0 + n_2 I(t)$

The refractive index is also wavelength dependent and a long wavelength travels faster through the material compared to a short wavelength. Since the pulse contains many different wavelengths it will experience different refractive indices resulting in this additional *temporal broadening* of the pulse.

It is very important that the pulse is broadened in such a way, that it is re-compressible in order to create a pulse with a good temporal shape. Avoiding non-linear effects as well as selecting the central part of the beam with a pinhole (because that is where the spectral broadening is the biggest) helps to create a good pulse shape. Unfortunately the use of a pinhole leads to a severe decrease of the transmitted energy and it has been suggested that a solution to this might be to couple the beam after the pinhole into a hollow wave-guide in vacuum and in this way keep most of the energy.

The idea of using bulk materials for post compression of ultrashort laser pulses was first suggested by *C. Rolland and P. B. Corkum* [1] in 1988 and then also discussed by *Petrov et al* in 1989 [3]. In 1998 *Diddams et al* [2]published a paper on how to characterize ultrashort pulses travelling through a bulk and much of the information in that paper is used during the work in this Master Thesis. The conditions for the focusing can be set up in such a way that the variation of the lasers diameter over the bulks material length is rather small and then similar conditions to those for optical fibers/capillaries can be achieved. The beam diameter can be quite large, since no

focusing into a fiber or capillary is needed, and hence the energy can be increased several orders of magnitude compared to that in fibers/capillaries. The intensity can be increased up to a certain limit and above this limit non-linear effects occur such as continuum generation and self-focusing, which make the pulse incompressible and may damage the bulk material.

The bulk is in fact common optical glasses, such as BK-7, SF59 and Fused Silica, in which the dispersion is significant. There are many other dispersive materials but in this Master Thesis only glass materials used during the experiments are mentioned.

When the laser beam has gone through the bulk it is collimated by a spherical mirror and sent into the compressor. The compressor is usually made of a pair of gratings or a prism pair and in our case the latter is chosen. In the prism compressor the short wavelengths travel faster than the long wavelengths, which is opposite to the case with the bulk material, and thus the pulse is compressed. The pulse is then sent to the autocorrelator for measurement of the pulse duration.

1.3 The goal of this Master Thesis

The goal of this Master Thesis is to produce an external pulse compression system with a bulk material at the 1 TW Titanium Sapphire laser at CELIA (Centre Lasers Intenses et Applications), Université Bordeaux 1. The 1 TW Titanium Sapphire laser at CELIA produces approximately 30 fs long pulses around the wavelength 804 nm and with a repetition rate of 1 kHz. The energy in each pulse can be as high as 20 mJ, but in the experiments done in this Master Thesis only a part of the main beam is used.

As a dispersive medium a bulk of BK-7 (an optical glass material) is used. The bulk is inserted in the laser beam close to focus in order to get broadened pulses with a positive linear chirp. After the bulk the central part of the beam is selected with a pinhole of various sizes. The beam is then collimated after the pinhole by a focusing mirror. The pulses are sent through a prism compressor (a pair of prisms), which compresses the pulses by removing the linear chirp. The goal is to get a pulse duration of approximately 10 fs.

1.4 Outline

Chapter two, *Theoretical background and calculations*, contains a more extensive explanation of the principle of post compression including Self Phase Modulation (SPM), Group Velocity Dispersion (GVD) and the combined effect of them. Chapter three, *Experimental set-up*, includes a description of the different parts of the set-up as well as a discussion of values for the best set-up and figures of the set-up on the table. The experimental results are presented and discussed in chapter four, *Results*. Conclusions that can be drawn from the experiments and outlooks for the future are collected in chapter five, *Conclusions and outlooks*. In chapter six, *Acknowledgements*, you will find the acknowledgements to all (I hope) people that have helped me during the work of this Master Thesis. Chapter seven contains the *References*. Finally, chapter eight contains the *Appendices*, which includes extra readings on *Gaussian Beams*, *The Non-linear Schrödinger equation* and *Autocorrelators*.

2 Theoretical background and calculations

2.1 Chirp

The electric field of a laser pulse can be represented by cosine functions and the field is then given by:

$$\overline{E} = \sum_i \overline{E}_i \cdot \cos(\omega_i t - k_i x + \varphi_i) \tag{3}$$

where the index *i* labels all the frequencies needed to describe the laser pulse.

A typical approximation of a laser pulse is the Gaussian distribution and the pulse is said to have a Gaussian pulse shape, the pulse is shown in Figure 2. The phase difference (phase shift), $\Delta\varphi$, in-between the neighbouring frequencies in a transform-limited pulse is equidistant. However, when the phase difference varies linearly with the frequency, i.e. with the index i in eq. (3) above, the pulse is said to have a *linear chirp*. The pulse can of course have a more complicated phase difference and then the chirp is non-linear. A linear chirp makes it easier to achieve good pulse compression and this is the chirp that is discussed in this Master Thesis.

Equation (1) suggests that an increase of the transform-limited pulses bandwidth results in a decrease of the pulse duration. The problem is that the pulse has to be transform-limited and this is not possible to achieve in real materials. All real materials are dispersive and introduce a positive chirp on the pulse and the best thing to do is to make the chirp a controllable parameter, by making sure that the chirp is *linear*. Figure 3 below shows a Gaussian pulse with a positive and linear chirp

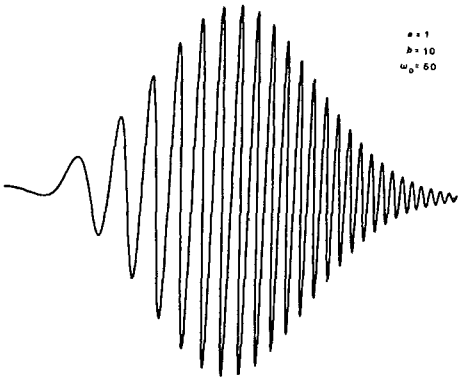

Figure 3. *A chirped Gaussian signal pulse (Figure 9.1 from [4]).*

The broadened pulse with linear chirp is then sent through a compressor, which introduce a negative linear chirp on the pulse and the result is a transform-limited pulse with shorter time duration.

2.2 Group velocity dispersion (GVD)

All real materials have a certain amount of dispersion and a dispersive system is any linear system for which the propagation constant, $\beta(\omega)$, is a function of frequency and can be described as a Taylor expansion. The propagation constant is in the literature also called the *wavevector, k*. In this Master Thesis the variable β is used and referred to as the propagation constant, given by

$$\beta = \frac{2\pi\, n(\omega)}{\lambda} \tag{4}$$

where $n(\omega)$ is the refractive index. Since the refractive index is frequency dependent so is the propagation constant and as long as the spectral width is quite narrow the frequency dependence can be expressed as a linear function

$$\beta = \beta_{\omega_0} + \left(\frac{\partial \beta}{\partial \omega}\right)_{\omega_0} (\omega - \omega_0) + \cdots \tag{5}$$

which is a Taylor expansion around the central frequency ω_0. For all reasonably narrowband pulsed or modulated signals it is sufficient with a first order expansion. But, if the pulses are really short, like in the ultrashort pulse region, the spectral width is quite broad and then the linear approximation is not sufficient anymore. Additional terms must be included in the Taylor expansion and thus the propagation constant becomes

$$\beta = \beta_{\omega_0} + \left(\frac{\partial \beta}{\partial \omega}\right)_{\omega_0} (\omega - \omega_0) + \frac{1}{2}\left(\frac{\partial^2 \beta}{\partial \omega^2}\right)_{\omega_0} (\omega - \omega_0)^2 + \frac{1}{6}\left(\frac{\partial^3 \beta}{\partial \omega^3}\right)_{\omega_0} (\omega - \omega_0)^3 + \cdots \tag{6}$$

For convenience the terms in the Taylor expansion of β are now denoted $\beta_1 = \partial\beta/\partial\omega$, $\beta_2 = \partial^2\beta/\partial\omega^2$ *and* $\beta_3 = \partial^3\beta/\partial\omega^3$. If the pulses are indeed very short further terms have to be included in the Taylor expansion of β and these higher order terms are referred to as *higher order dispersion*, which are discussed in chapter 2.6.

The β_1 term is the inverse of the *group velocity*, v_g. The group velocity is the velocity with which the whole pulse travels forward

$$v_g = \left[\left(\frac{\partial \beta}{\partial \omega}\right)_{\omega=\omega_0}\right]^{-1} \tag{7}$$

However, the individual optical frequencies within the pulse move forward with the *phase velocity*, φ_g.

The second order term β_2 corresponds to the *group velocity dispersion* (GVD). The physical interpretation of GVD is that the group velocity, v_g, is varying with frequency since different wavelengths travel with different velocities through the material and this makes the pulse temporally longer.

The time delay (due to GVD) after a distance z is given by [5]

$$\Delta\tau \approx z\left|\left(\frac{\partial^2 \beta}{\partial \omega^2}\right)_{\omega_0}\right| \Delta\omega \tag{8}$$

Depending on the sign of the GVD term the dispersion is either positive or negative. Most common materials have positive GVD, $\beta_2 > 0$,and this gives the leading edge lower and the trailing edge higher frequencies.

If GVD is the only mechanism affecting the pulse it will acquire a *linear* chirp. The type of broadening resulting from GVD becomes increasingly important for pulses in the picosecond and femtosecond regions and after only a few mm of propagation in the material.

The broadened pulse duration is given by [4]

$$\tau_1^2(z) = \tau_0^2 + \left(\frac{(4\ln 2)\beta_2}{\tau_0^2} z \right)^2 \quad (9)$$

and by introducing the dispersion length, z_D, it can be simplified to

$$\tau_1 = \tau_0 \sqrt{1 + \left(\frac{z}{z_D} \right)^2} \quad (10)$$

where τ_0 is the initial pulse duration. This shows that the effect of *GVD* increases with the thickness of the material. The *dispersion length*, z_D, is the distance to the point where the unchirped input pulse width has increased with a factor $\sqrt{2}$

$$z_D \equiv \frac{\tau_0^2}{(4\ln 2)\beta_2} \quad (11)$$

2.3 Self Phase Modulation (SPM)

The non-linear part, n_2, of the refractive index expressed in equation (2) is theoretically given by:

$$n_2 = \frac{12\pi^2}{n_0^2 c} \chi^{(3)} \quad (12)$$

where the last term is the third order susceptibility. The *Kerr effect* with a positive sign, $n_2>0$, is present in most optical materials and in optical glass such as BK-7 or Fused Silica the expected values are around $n_2 \approx 10^{-16}$ cm^2/W.

A variety of propagation effects results from the Kerr effect and one of them is the *self-phase modulation* (SPM). In order to get SPM the non-linear part of the refraction index has to be significant and also the amplitude of the intensity has to be sufficiently high. The addition to the refraction index due to the intensity dependence must result in a significant increase in the optical path length, $n \cdot L$, travelled by the pulse, at least near the peak of the pulse. The medium gets optically longer which results in a delay of the optical cycles as well as creation of new frequencies. The refraction index becomes time dependent (through $I(t)$) which affects the pulse. After the influence of SPM the spectrum is shifted to lower frequencies at the leading edge while the central part is unaffected and the trailing edge is shifted towards higher frequencies. In other words, the leading edge shifts towards the red and the falling edge towards the blue region.

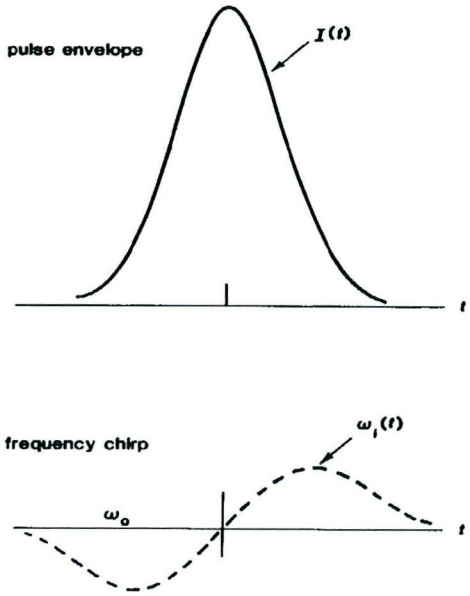

Figure 4. The initial effect of intensity dependent SPM is to lower the frequency on the leading edge and raise the frequency on the trailing edge of the pulse, thus producing a linear chirp at the centre of the pulse. (Figure 10.12 from [4])

The phase is given by

$$\varphi(t) = \omega_0 t - \varphi_2(t) = \omega_0 t - \beta z = \omega_0 t - \frac{\omega_0 n_0}{c} z - \frac{\omega_0 n_2 I}{c} z \tag{13}$$

The frequency of the pulse is given by the time derivative of the phase and is thus also intensity and time dependent

$$\omega = \frac{d\varphi(t)}{dt} = \omega_0 - z \frac{\omega_0 n_2}{c} \frac{dI}{dt} \tag{14}$$

where $I = I(t)$ and ω_0 is the current pulse frequency. This expression indicates that new frequencies are created due to the intensity and time dependence.

Thus $\omega = \omega(t)$ is dependent of the time derivative of the light intensity and for a bell shaped pulse, such as a Gaussian, the phase $\varphi = \varphi(t)$ changes with time. Consequently, the frequency varies with time and the *chirp* induced by the SPM is given by

$$\Delta\omega(t) = \omega(t) - \omega_0 \tag{15}$$

It is interesting to know at which distance through the bulk the maximum phase shift, φ_{max}, is obtained in order to optimise the experimental set-up. This parameter is called the *Non-linear length*, z_{NL}, and defined as

$$z_{NL} = \frac{1}{\gamma P_0} \tag{16}$$

where

$$\gamma = \frac{n_2 \omega_0}{c A_{eff}} \tag{17}$$

γ is called the *non-linear coefficient*, P_0 is the peak power, ω_0 is the central frequency and A_{eff} is the *effective beam area*. The physical interpretation is that the maximum phase shift is $\varphi_{max} = 1$ when the pulse has propagated the distance z_{NL}. When only the SPM is taken into account the NLSE equation, see equation (40) in appendix 8.2, is reduced to

$$\frac{dE}{dz} = \frac{i}{z_{NL}} E \tag{18}$$

The maximum phase shift after a distance z is approximately

$$\varphi_{\max} = \frac{z}{z_{NL}} \tag{19}$$

As mentioned in the introduction the compression of a spectrally broadened pulse is greatly enhanced if the chirp is linear. If only pure SPM affects the pulse the chirp is not linear. However, if SPM acts together with GVD the chirp can become linear and the re-compression will not be so difficult.

2.4 Combined effect of SPM and GVD

As previously mentioned, the SPM produces low frequencies in the leading edge of the pulse and these low frequencies will travel faster through the material than the high frequencies in the trailing edge, due to the GVD. It is evident that the contribution from SPM is largest on the slopes of the pulse, since the expression for the SPM includes *dI/dt*. However, the flat parts of the pulse are not affected at all since there is no change of intensity. Thus the combined effect of SPM and GVD is largest on the sides of the pulse and the combination of them results in a spectral broadening on the sides, which in turn leads to a pulse shape resembling a square pulse with an almost linear chirp. The combination of SPM and GVD stretches the pulse faster than if only GVD was to act alone and the combination can result in at least three types of behaviour, [4]

1) Broadening and enhanced frequency chirping
2) Severe pulse distortion and break up
3) Soliton formation and propagation

of which only (1) is studied in this Master Thesis, since that is the basic idea of post compression. An ideal pulse with a smooth profile without distortions will with a combination of SPM and GVD get an almost linear frequency chirp.

A linear chirp is very important, because if a pulse has a linear chirp (positive or negative) it can be sent through a system with the opposite GVD in order to be compressed to shorter pulse duration than the original pulse. A pulse with a linear chirp keeps a pretty nice temporal shape even after compression in an experimental set-up.

The pulse duration becomes longer when both SPM and GVD are allowed to work on the pulse since the GVD stretches the pulse and thereby slightly decreases the effect of the SPM [5]. But, on the other hand GVD, leading to a reduced peak intensity, is necessary in order to get a *linear* chirp.

Depending on the parameters of the input pulse, there is an *optimum material length*, z_{opt}, of the bulk for which the compression is most effective. As discussed before, only a proper combination of SPM and GVD will result in an almost linear chirp, which means that the optimum length of the material, z_{opt}, is a combination of the dispersion length z_D and the non-linear length z_{NL}. In [9] the combination of the dispersion length and the non-linear length has been numerically examined for the fiber case and for bulk materials it is approximately the same as long as the non-linear and dispersion lengths are small

(21) $$z_{opt} = 1{,}4 \cdot \sqrt{z_D \cdot z_{NL}}$$

The z_{opt} has to be shorter than the *confocal length*, L_c, which is twice the Rayleigh distance, z_R (see chapter 8.1)

(20) $$z_{opt} < L_c = 2 \cdot z_R = 2 \cdot \frac{\pi w_0^2}{\lambda}$$

The *compression factor*, S, is a number of the system's ability to compress the incoming pulse and it is defined as

(22) $$S = \frac{\tau_0}{\Delta\tau}$$

where τ_0 is the input pulse duration while $\Delta\tau$ is the averaged re-compressed pulse duration after the pulse compression system. The compression factor can be shown to be independent of the bulk material's dispersion in contrast to the fiber case.

2.5 Self-Focusing (SF)

As discussed before, the wave's velocity depends on the wave intensity since the velocity through the material depends on the refraction index. When the *optical Kerr effect* appears the wave undergoes SPM as well as *self-focusing* (*SF*) at high energy, see Figure 5 below.

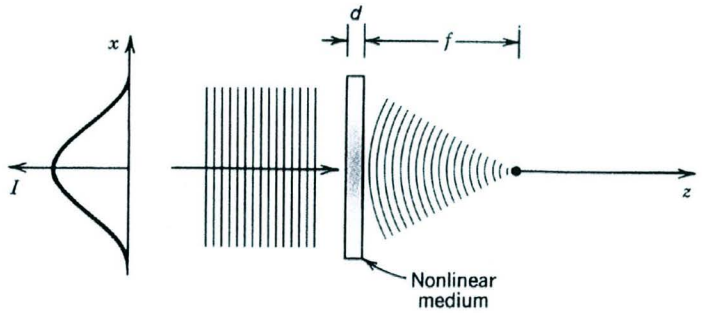

Figure 5. A third-order non-linear medium acts as a lens whose focusing power depends on the intensity of the incident beam. (Figure 19.3-2 from [4]).

SF can occur when the incident beam has a nonuniform transverse intensity distribrution and the non-linear refraction index, n_2, is positive. Under these conditions the bulk material acts like a positive lens, as can be seen in Figure 5. SF occurs definitely if the power of the input beam, P, is greater than a critical value P_{crit}, but will not occur if the power is less than P_{crit}. The critical value for Gaussian beams is given by [6]

$$P_{crit} = \frac{\pi (0{,}61)^2 \lambda^2}{8 n_0 n_2} \tag{23}$$

which is independent of the beam diameter. It is important to remember that it is the power and not the intensity that determines whether SF will occur or not. Due to SF the pulse will decrease its diameter while travelling through the material until reaching a minimum (focus) at a distance called the *SF length*, z_{sf}, which is given by [6]

$$z_{SF} = w_0^2 \sqrt{\frac{\pi n_0}{2 n_2 P}} \tag{24}$$

where

$$P = \frac{1}{2} \pi w_0^2 I_0 \tag{25}$$

and w_0 is the beam waist and I_0 is the maximum intensity of the input beam.

In order to avoid Self Focusing it is important that the optical material length is smaller than z_{SF}. Calculations of z_{opt} and z_{SF} are found in Table 1 and Table 2 in chapter 2.8 and the conclusion is that it is not needed to take self focusing into account since the length is much longer than for optimum spectral broadening.

2.6 Higher order effects

The higher order effects described in this chapter are not taken into account in the calculations or in the experiments during the work on this Master Thesis, since they are believed to not be of major importance at the pulse durations used in the experiments. The effects are briefly discussed in the following sections.

2.6.1 Third order dispersion (TOD)

The importance of the third order dispersion increases when the pulses get shorter. The third order dispersion corresponds to the fourth term in the expression for the wave number β

$$\beta_3 = \left(\frac{\partial^3 \beta}{\partial \omega^3} \right)_{\omega_f} \tag{27}$$

When the pulses are sufficiently short, less than 10 fs, this term has to be added to the NLSE, eq. (40). According to [5] the third order dispersion has to be added when the dispersion length z_D and $z_{D2} = \tau_0^3/|\beta_3|$ are of comparable magnitude or when the GVD is close to zero. TOD broadens the pulse, but not symmetrically, as compared to GVD, and the trailing edge will get longer and modulated, see [5].

2.6.2 Response time of the media

Depending on the media the response time due to optical polarization will be different. There are two kinds of polarization; electronic polarization and molecular

orientation. The response time depending on the electrons is much shorter that the time depending on the molecular orientation. The molecular response time depends on the media and can according to [8] be anything from $t_R \approx 50$ fs to more than 1 ps.

Nonresonant electronic non-linearities occur as a result of the non-linear response of bound electrons in the bulk material. The response time corresponds to the required time for the electron cloud to be distorted due to an applied optical field. An estimation of the response time with respect to the Bohr model of the atom is

$$\tau = \frac{2\pi a_0}{v} \approx 10^{-16} s \tag{28}$$

where a_0 is the Bohr radius and $v = c/137$ according to [6].

If the response time is of the same order of magnitude as the pulse duration it has to be included in the calculations of the NLSE and will then lead to a red shift and additional modulations of the pulse. Though if the response time is much longer or much shorter than the pulse duration it does not affect it significantly and there is no need to include it in the calculations. The latter is the case in this Master Thesis.

2.6.3 Self steepening

Self steepening acts like a kind of intensity dependent GVD and when it affects a pulse the part with the highest intensity will travel slower than the parts with lower intensity. This leads to a kind of steepening effect on the trailing edge of pulse. The parameter for self steepening is given by [5]

$$s = \frac{2}{w_0 \tau_0} \tag{29}$$

and is included in the non-linear Schrödinger equation (see appendix 8.2). The self steepening has an effect on the SPM, the broadening in the blue region is increased, compared to a pulse not affected by it and the resulting spectrum is very asymmetric, for more information and expressions see [5].

2.7 Pulse compression

The broadened pulse with a positive linear chirp is compressed by travelling through an optical set up, called compressor, which affects the pulse with a negative linear chirp. In other words, a compressor with a negative GVD. The compressor normally consists of either two gratings or a prism pair. In this Master Thesis a prism pair is used and it is described in more detail in chapter 3.2.

2.8 Calculated results for different materials

In Table 1 are the values for the refraction indices gathered for different materials. Please note that the values of n_2 for SF-59 and SF-10 are only estimates.

Material	$\mathbf{n_0}$ (at λ=804 nm)	$\mathbf{n_2}$ / [$\cdot 10^{-20}$ $\mathbf{m^2/W}$] (at λ=804 nm)
BK-7	1,51	3,75
SiO_2 (Fused silica)	1,45	2,48
SF-59	1,98 (at 800 nm)	17,4 (*)
SF-10	1,71	70,0 (*)
Sapphire	1,75 (e) / 1,76 (o)	3,10
MgF_2	1,38 (e) / 1,39 (e)	1,15

Table 1. The approximate values of the linear and the non-linear part of the refraction index for different optical materials. (*) There is a big uncertainty in the value of n_2 for SF-59 and SF-10, since it is just a very rough estimate. The SF-59 and SF-10 are known to be highly dispersive materials.

In Table 2 the dispersion length (z_D), non-linear length (z_{NL}) optimum material length (z_{opt}) and the SF length (z_{SF}) are tabulated for different optical materials. The refraction index is calculated at the wavelength 804 nm and with a input pulse duration of 30 fs.

Material	z_D / [mm] GVD	z_{NL} / [mm] SPM	z_{opt} / [mm] both GVD and SPM	z_{SF} / [mm] Self Focusing
BK-7	7,20	2,72	6,20	82,9
SiO_2 (Fused silica)	8,84	4,11	8,44	100
SF-10	2,01	0,587	1,52	41,0
Sapphire	5,51 (o) / 5,65 (e)	3,29	5,96 (e) / 6,04 (o)	98,5
MgF_2	15,6 (e) / 16,2 (o)	8,87	16,4 (e) / 16,7 (o)	≈ 143

Table 2. Values of the dispersion length z_D, non-linear length z_{NL}, optimum thickness z_{opt} and the SF length z_{SF} for different optical materials. The central wavelength is $\lambda = 804$ nm and the pulse duration of the incoming pulse is $\tau_0 = 30$ fs.

The conclusion from Table 2 is that there is no problem with Self Focusing effects in the bulk since the SF length is considerably longer than the optimum material lengths.

3 Experimental set-up

3.1 The terawatt laser at Celia

The 1 TW Titanium Sapphire laser at CELIA can produce approximately 30 fs long pulses around the wavelength 804 nm and with a repetition rate of 1 kHz. The energy in each pulse can be as high as 20 mJ, but in the experiment done in this Master Thesis only a part of the main beam was used with a maximum energy of 670 μJ resulting in peak powers around 20 GW. Beam energies of around 500 μJ were normally used in order to be able to reproduce the results on a day-to-day basis.

3.2 Overview of the experimental set-up

Figure 6 is an overview of the guiding of the main laser beam at the CELIA Terawatt laser facility through the splitting and guiding to the experimental set-up used in this Master Thesis.

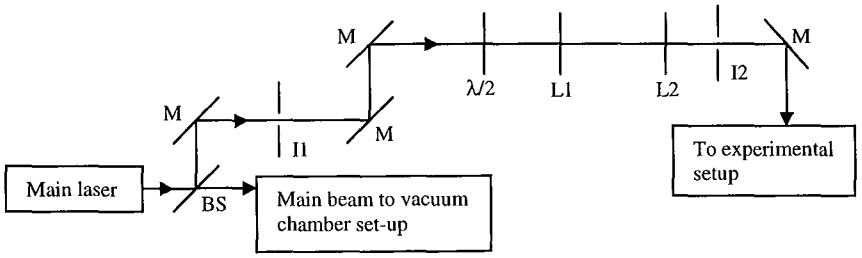

Figure 6. Dividing of the main beam by a beam splitter, collimation and guiding over to the experimental set-up. Around 10 % of the main beam is reflected by the beam splitter, BS, then the beam is guided by the first three mirrors via an iris I1 (ϕ_1 = 2,5 mm) to the half wave plate, λ/2, which is used to change the energy of the beam. The lenses L1 (defocusing) and L2 (focusing) collimate the beam. The beam passes by an iris, I2 (ϕ_2 = 12,5 mm), and is then reflected by the last mirror to the experimental set-up.

The pulse compression experiments use only a small part of the original beam from the terawatt laser. The beam is extracted using a beam splitter and then sent to the experimental set-up where it is characterized and used in the bulk experiments. The selection of the beam and the guiding is done according to Figure 6 above. The beam splitter is made of BK-7 and reflects around 10% of the incident light at λ = 800 nm.

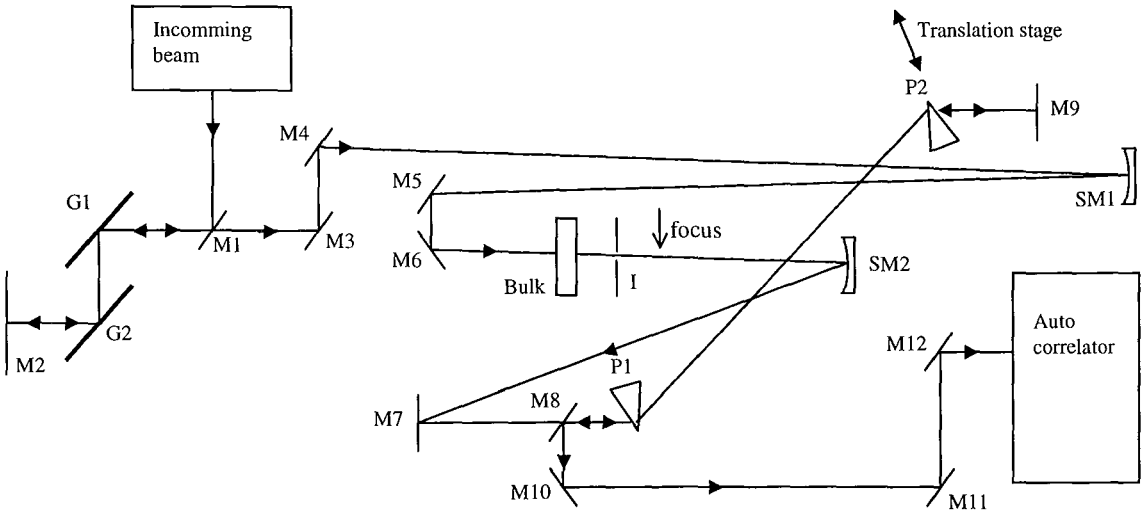

Figure 7. The experimental setup on the table seen from above.

The beam is sent by M1 into the grating pre-compressor G1-G2 and the beam is at a higher level depending on the folded mirror M2. The gratings work together as a pre-compressor and the compressor is adjusted to get a short pulse, around 30 fs, in the experimental set-up. However, in a second series of experiments the pre-compressor is adjusted to pre-compensate for the chirp that is induced by the bulk. After the pre-compressor the beam is directed by the mirrors M3-M4 onto the spherical focusing mirror SM1 (f_1 = 3 m) with a long focal length in order to get a slowly converging beam. Then the beam is directed onto the bulk (non-linear material) and the central, most broadened part of the beam is selected with a pinhole, I. The pinhole makes the beam divergent and in order to collimate it the spherical focusing mirror SM2 is inserted with the pinhole at its focal point (f_2 = 0,5 m).

The mirror M8 is inserted at an angle close to 45° and has a hole in it in order to let the beam through to the prism compressor, P1-P2 and M9. The beam enters P1 close to the edge and almost at the bottom of it. The beam passes through to the second prism, P2 and then to the mirror M9. The mirror M9 consists of two mirrors mounted on a holder at an angle of 90° in-between them in order to translate the beam to a higher level. The beam has to be at a higher level in order to extract the compressed pulse at the output of the prism compressor, since the output is at the same position as the input. At the output the beam is on a higher level than before and is now reflected from M8 to M10 and then directed via M11-M12 to the autocorrelator.

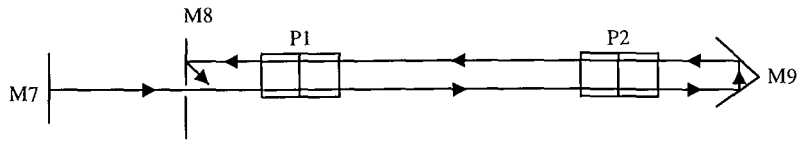

Figure 8. The prism compressor viewed from the side.

The prism compressor consists of two fused silica prisms with an deviation angle of 60°. The prisms are put vertically in the beam line so that the beam experiences minimum deviation, as shown in Figure 8. The incident angle at the first prism (P1) is the Brewster angle, which minimizes the reflection losses. Minimum deviation is obtained by putting the first prism into the beam line and then rotate it until the minimum deviation from the original beam line is found.

3.2.1 Beam focus

A spherical mirror, SM1 in Figure 7, with a focal length of 3 meters, focuses the beam. At 500 μJ there is severe continuum generation at the focus and this can be seen and heard directly when moving a piece of paper in the beam.

The beam radius as well as the beam waist are measured by inserting pinholes of different sizes in the beam at several positions after SM1 and then measuring the transmitted energy. The equation for a Gaussian beam, see appendix 8.1, is fitted to the experimental data and the *beam spot size*, w, is calculated as the value that makes the fitted graph correspond the best with the experimental data. The *beam waist*, w_0, is then calculated.

In Figure 9, some experimental data as well as the fitted graph of a Gaussian beam are shown. The experimental and theoretical values seem to fit well together and results are looked upon as quite reliable. Also, the measurements are done several times and the results are approximately the same every time.

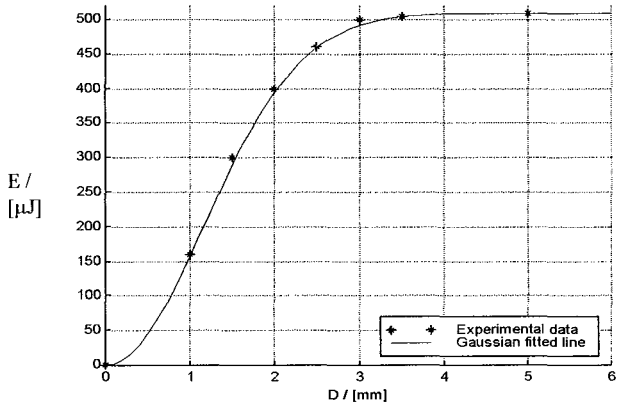

Figure 9. The measured energy data and the fitted theoretical energy curve. The beam size at the measuring position is calculated from the fitted data to $w \approx 1{,}16$ mm and the beam waist is estimated to $2w_0 \approx 0{,}7$ mm.

The measurement of the beam radius is done at the energy $E_{max} = 510$ μJ and at position 6, see Table 3 for more info about the positions. The beam spot size at this position is then calculated, from the fitted data, to $\boldsymbol{w \approx 1{,}16}$ **mm** and the beam waist is estimated to $\boldsymbol{2w_0 \approx 0{,}7}$ **mm**.

The bulk is placed at different positions in the set-up and in Table 3 these positions are related to mirror M6 in the overview of the set-up, see Figure 7. The reason to why the positions are measured from the mirror and not the focus is due to the difficulty in positioning the focus. The positions are before focus, which is approximately one meter from the mirror M6 at position 13, see Figure 7.

Position / [cm]	**1**	**2**	**3**	**4**	**5**	**6**	**7**	**8**	**9**	**10**	**11**	**12**	**13**
Distance in cm from the last mirror, M6, to focus	11	19	26,5	34	41,5	49	56,5	64	71,5	79	86,5	94	101,5

Table 3. Positions for the bulk. The positions are measured in centimetre from the last mirror, M6, before focus.

3.2.2 *Power and beam size*

The pulse duration of the input beam is $\tau_0 \approx$ **30 fs** and for the input energy E_0 = 450 μJ, the intensity and power is

$$I = \frac{E_0}{\tau_0} \cdot \left(\frac{2}{\pi w^2} \right) \approx 700 \text{ GW/cm}^2 \quad (30)$$

$$P = \frac{E_0}{\tau_0} \approx 15 \text{ GW} \quad (31)$$

The goal is to get an intensity as high as possible in the material since then the most broadening will be achieved. But, at the same time effects such as continuum generation have to be avoided because if it is too strong the pulse will be irregular and difficult to compress.

3.2.3 *Selection with a pinhole*

A pinhole is inserted directly after the bulk in order to select the part of the beam with the broadest bandwidth, which is at the centre. The pinhole is mounted on a holder that is movable in both the horizontal and vertical planes. The central region of the beam is found by moving the pinhole until the maximum intensity is seen on a screen placed behind it. Finer adjustments are done by watching the spectrum from the spectrometer, which is displayed on the computer screen, and try to move the pinhole until the broadest bandwidth is obtained. Since the spectra are very different from sample to sample this adjustment takes a lot of time and it is hard to decide when the best position is reached. The pinholes used here have a diameter of either ϕ=150 μm or ϕ=400 μm. A drawback with the pinhole is its low energy transmittance.

3.3 *Optimisation of the set-up*

3.3.1 *Pinhole dimension*

With a 150 μm pinhole the transmitted energy is 3% (≈14 μJ) compared to a 400 μm pinhole, which transmits 10% (50 μJ). A pinhole of 1 mm leads to an increase of pulse duration. Unfortunately pinholes with a diameter 400 μm < ϕ < 1 mm is not available.

3.3.2 *Selection of bulk material and thickness*

The spectral broadening for several different optical glasses (bulks) and dimensions are tested in order to find the best combination of thickness and beam intensity. The bulk is moved along the beam line and the pinhole is inserted behind the bulk. The broadening for different materials in the positions along the beam from mirror M6 to focus is collected in Table 4. The input energy is E = **450** μ**J**, the pinhole diameter ϕ = **150** μ**m** and without bulk material the bandwidth is $\Delta\lambda \approx$ **35 nm**.

Material	$\Delta\lambda_1$/ [nm]	$\Delta\lambda_2$/ [nm]	$\Delta\lambda_3$/ [nm]	$\Delta\lambda_4$/ [nm]	$\Delta\lambda_5$/ [nm]	$\Delta\lambda_6$/ [nm]	$\Delta\lambda_7$/ [nm]	$\Delta\lambda_8$/ [nm]	$\Delta\lambda_9$/ [nm]	$\Delta\lambda_{10}$/ [nm]
SiO_2	39	39	39	39,5	41,5	42	42,5	46	49 (*)	X
BK7 3mm	35	35	34	36	35,5	36,5	36,5	39,5	41	42 (**)
BK7 6mm	40	40	41	40,5	44	46	49	51	51	54 (*)
BK7 11mm	39	40	40	41	42	47,5	49,5	51 (*)	X	X
SF-59	46	46	49	49	50	50	50	X	X	X

Table 4. Bandwidth at different distances from focus for different bulk materials, the index of $\Delta\lambda_1$ correlates to the numbers of the positions in Table 3. (*)Very close to continuum generation. The spectrum has got a very unpleasant top to the right, which could be due to continuum generation in the bulk. (**) The energy in the beam focus results in non-linear effects in the air. This makes it very hard to place the pinhole at a good spot. It did not seem to matter though since the bandwidth was not very big anyway.

The crosses in Table 4 means that the bulk cannot be inserted at that position due to too much continuum generation and in the case of SF-59 the material is severely damaged if it goes any closer to focus than position 7. The data from Table 4 is plotted in a graph below to visualise the results, see Figure 10. The distance between the gratings in the pre-compressor is not changed, which means no pre-compensation of the chirp. Experiments with pre-compensation of the chirp are done later.

From Figure 10 the conclusion is that most of the tested materials will reach a spectrum with a FWHM of 50 nm when it is sufficiently close to focus. It is not totally clear from the figure which material should be used. Even though SF-59 is the most dispersive of the materials it should not be chosen since it is severely damaged already after this experiment, in which the energy was not maximised. Besides, any of the other materials seem to get up to the same broadening. In order to choose a suiting material additional theoretical calculations are done as a comparison to the experimental results.

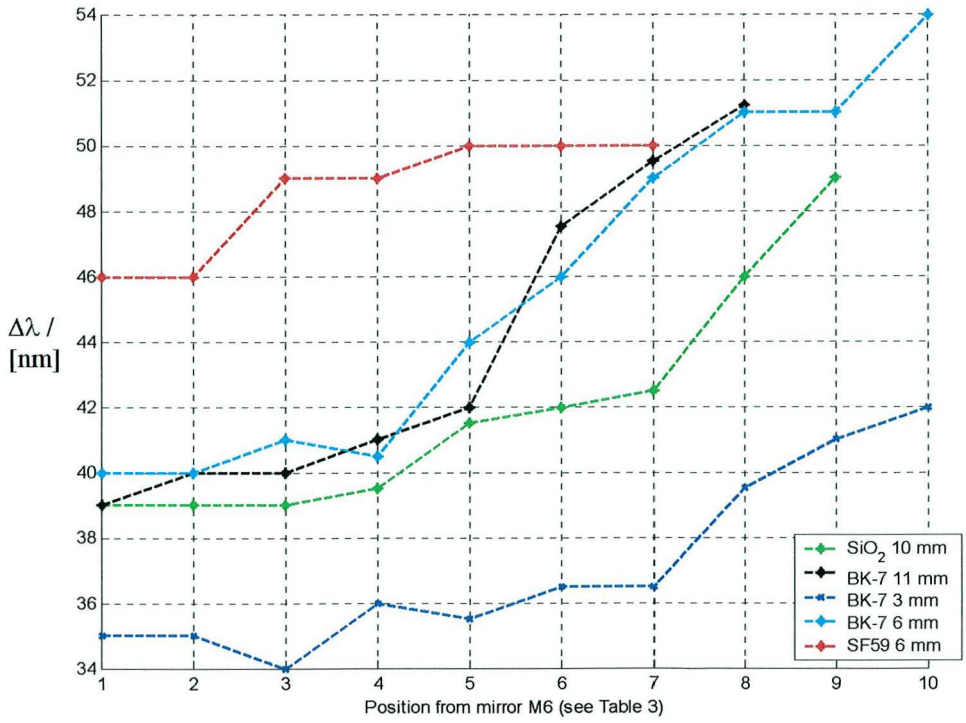

Figure 10. The bandwidth, $\Delta\lambda$, as a function of the position according to Table 3 for different materials. The distance increases the further from the mirror M6 the bulk is placed. The blue line with stars is 6 mm SF-59, the red line with stars is 1 cm SiO_2 (Fused Silica), the black line with crosses is 11 mm BK-7, the blue line with crosses is 3 mm BK-7 and the line with the colour magenta and crosses is 6 mm BK-7. The distance between the gratings in the pre-compressor is not changed, which means no pre-compensation of the chirp.

Taking all the calculated and measured results into account, the chosen bulk is the optical glass BK-7 with thickness d = **11 mm** and diameter ϕ = **5 cm**. Note that, according to the theoretical calculations in Table 2 the 6 mm dimension would be a better choice. The bulk is placed before focus at position 8, see Table 3, where it yields the biggest spectral broadening, but this is valid only when the pulse is not pre-compensated for the chirp induced by the bulk, see chapter 3.3.3.

3.3.3 Pre-compensation of the chirp

When the incident pulse has the shortest pulse duration possible, τ = 28 fs, the spectrum is $\Delta\lambda \approx$ 35 nm and the maximum broadening is according to Table 4 at position 8 with $\Delta\lambda$ = 51 nm. However, at this position there is some continuum generation in the material. Pre-compensation of the chirp can now broaden the spectrum even more but then the position of the working spot has to be changed since the intensity changes too.

When pre-compensating for the chirp, the spectrum becomes broader and the pulse duration is enlarged. The pre-compressor consists of two optical gratings on translation stages and both the distance in between the gratings, as well as the angle between the surfaces can be changed. The pulse's chirp is depending on the distance between the gratings and when the pulse duration is as short as possible the pulse has no chirp. By moving the gratings the pulse is linearly pre-compensated for the chirp. The broadest spectrum is found experimentally by a combination of moving the bulk to different positions, optimise the distance of the gratings and at the same time check the spectral width.

Concerning the positions it is important that the intensity is not too high but sufficient in order to get the non-linear part of the refraction index to be of importance. Though, too high intensity produces serious self-focusing effects and continuum generation in the bulk and these are undesired effects that can make the pulse incompressible because of major irregularities. The continuum generation also makes the bandwidth considerably smaller and alters the pulse shapes from shot to shot and that should be avoided.

It is noted that the biggest broadening appears at the edge of continuum generation. If the bulk gets any closer to the laser beam's focus the continuum generation makes the beam irregular and the self focusing effects makes the beam focus even more in air.

For the chosen bulk, 11 mm BK-7, the maximum broadening after the bulk is found to be $\Delta\lambda \approx$ **60 nm** at a pulse duration of $\tau \approx$ **150 fs**.

3.3.4 Optimisation of the prism compressor

The prisms in the prism compressor are inserted perfectly vertical into the beam and optimised for minimum deviation as explained above. The distance between the prisms is L_{prism} = 171 cm which means that the light travels twice that distance. In order to optimise the prism compressor the prisms were moved with a translation stage (a micrometer screw on the holder) while the output signal from the autocorrelator was studied with an oscilloscope. The optimum simply corresponds to the narrowest curve on the oscilloscope. In this set-up the beam passes through the very tip of the prisms.

3.4 Measurement of the pulse duration

The pulse duration is measured with a multishot autocorrelator containing a Type-1 BBO crystal with a thickness of 10 μm. The multishot autocorrelator uses several pulses to create the autocorrelation trace and this suggests that the pulses must be approximately regular and have the same appearance on a shot to shot basis. See chapter 8.3 for more information and theory about autocorrelators.

3.5 Measurement of the spectrum

The spectrometer is a single grating spectrometer in which the opening slit is attached to an optical fiber in order to enhance the availability of the spectrometer on the table. The output of the spectrometer is coupled to a computer and the spectrometer signal is displayed on the screen by the program Winspec. If the energy into the fiber is too high non-linear effects will appear within the fiber. In order to lower the energy input the fiber is directed towards the beam spot on a white A4-paper and hence the spectrometer input beam is only a weak reflection.

4 Results

4.1 Spectra

The shortest pulse duration is $\tau_0 \approx 28$ fs after the grating compressor and the bandwidth is $\Delta\lambda \approx 30$ nm. When the pulse passes the bulk severe continuum generation appears due to the very short pulse length and in order to avoid damaging the glass material the distance between the two gratings in the grating compressor is changed. The change of the distance between the gratings will pre-compensate for the chirp in the bulk. This makes the incoming pulse as long as $\tau_0 = 150$ fs and as the pulse passes the bulk also the bandwidth will increase with a linear chirp. Figure 11 depicts a spectrum before and after the bulk and the bandwidth is broadened by a factor of 1,7 – 2.

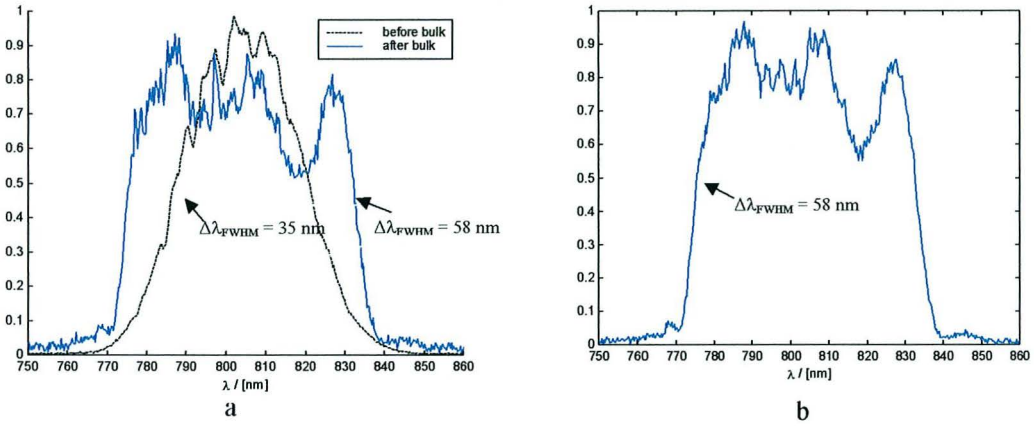

Figure 11. Spectra measured with the spectrometer. In a) before and after the non-linear material and in b) after the prism compressor. As shown in the diagrams, the spectra has approximately the same shape after the bulk material and after the prism compressor. The band width $\Delta\lambda = 58$ nm.

The pre-compensation for the chirp in the bulk material changes the pulse duration as well as the spectrum. At the position where the spectrum is as broad as possible the compression factor might also be as big as possible. However, continuum generation is always avoided because otherwise the pulses will be almost impossible to compress. The effect also result in quite narrow bandwidths, while the less severe continuum results in a increase of the bandwidth and the used pulses have after pre-compensation of the chirp a bandwidth of $\Delta\lambda \approx$ **59 nm** and a pulse duration of $\tau_0 \approx$ **150 fs**. In Figure 12 the bandwidth is shown as a function of the grating distance and the best choice is where the bandwidth is the broadest. In Figure 13 the corresponding spectra are depicted.

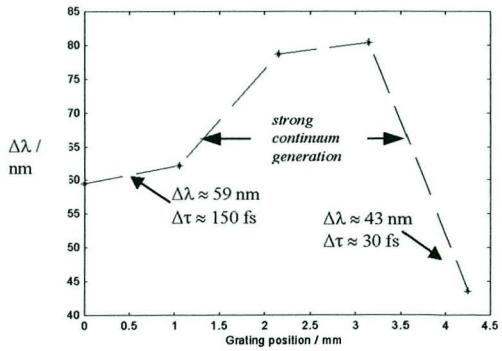

Figure 12. Bandwidth Δλ as a function of the increasing distance between the gratings. An increase of the grating distance decreases the output pulse duration from the grating compressor. Though, too short pulse duration creates continuum generation in the non-linear material. There is strong continuum generation and self-focusing after an increase of around 1mm and so forth.

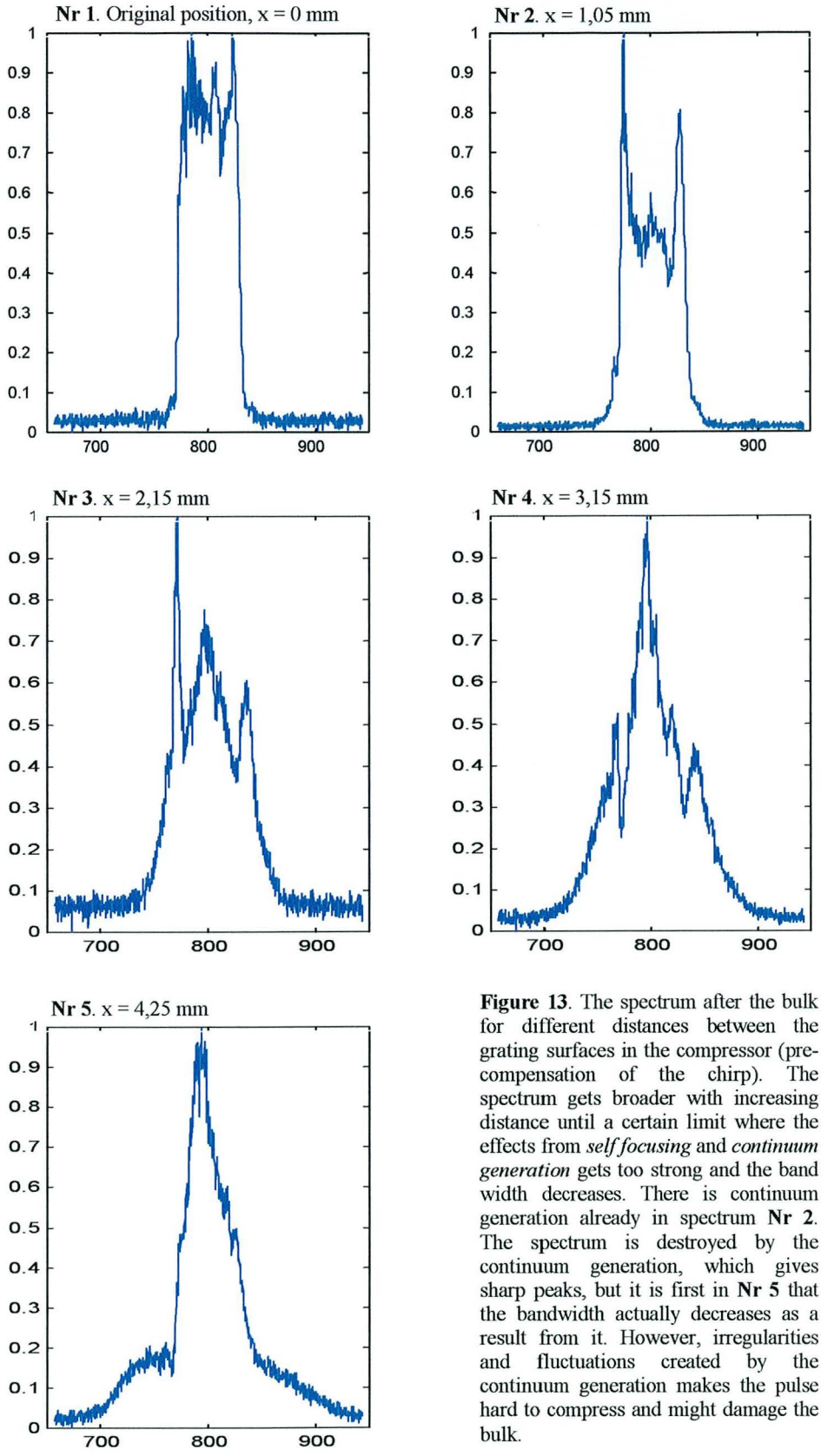

Figure 13. The spectrum after the bulk for different distances between the grating surfaces in the compressor (pre-compensation of the chirp). The spectrum gets broader with increasing distance until a certain limit where the effects from *self focusing* and *continuum generation* gets too strong and the band width decreases. There is continuum generation already in spectrum **Nr 2**. The spectrum is destroyed by the continuum generation, which gives sharp peaks, but it is first in **Nr 5** that the bandwidth actually decreases as a result from it. However, irregularities and fluctuations created by the continuum generation makes the pulse hard to compress and might damage the bulk.

A collimating spherical mirror (SM2 in Figure 7) is inserted in the laser beam at a distance of approximately 50 cm after the pinhole. Since it is a focusing mirror, with $f = 50$ cm, and not a lens there are no problems with astigmatism or dispersion in the material while the angle between the incident and the reflected beam is very small.

The transmitted pulse energy after a 150 μm pinhole is at the collimating mirror 3-4% (≈14 μJ) of the input energy, while a 400 μm pinhole transmits 10% (≈50 μJ). The input energy is 450 - 500μJ.

4.2 Pulse duration

After the prism compressor the pulse is sent to the multishot autocorrelator. The energy in the beam is far too high for the autocorrelator and has to be attenuated several orders of magnitude. Several optical filters are used for the attenuation and they do probably introduce some GVD that changes the laser pulse. However, the set-up is optimised with the filters present, so their possibly positive or negative effect are included in the measurements.

The laser pulses are measured by the autocorrelator and displayed on an oscilloscope screen. The signal on the oscilloscope is called the *autocorrelation trace*, $\tau_{ac\text{-}FWHM}$, and corresponds to the pulse duration, τ_{FWHM}, in the following way

$$\tau_{FWHM} = \frac{\tau_{ac-FWHM}}{a} \tag{32}$$

where a =1,414 for a Gaussian and a = 1,543 for a $sech^2$ pulse shape. Several series of pulses are measured and the average pulse duration is $\tau_{FWHM} \approx 14$ fs. The autocorrelator traces can be saved on the oscilloscope and the data is then transferred to MATLAB where the fitting of a $sech^2$ pulse shape is done. In Figure14 an autocorrelator signal as well as the fitted $sech^2$ pulse are shown.

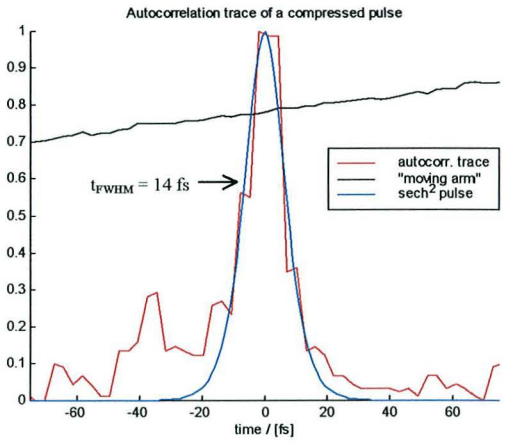

Figure 14. Autocorrelation trace for a compressed pulse. The pulse duration is 14 fs using a $sech^2$ pulse shape.

The shortest pulses produced are around $\tau_{FWHM} \approx 10$ fs with an energy of approximately 50 μJ. However, an uncertainty in this value is that the autocorrelator is at the edge of its resolution. The resulting compression factor is, for the shortest pulse, $\boldsymbol{S} = \mathbf{3}$.

5 Conclusions and outlooks

Ultrashort pulses can be used to a variety of applications such as

- Use the high pulse intensity in order to submit an atomic, molecular or solid system to an extreme electric field without destroying it and then study ultra fast dynamics with a time resolution in the femtosecond order of magnitude. Not destroying the system means no ionisation.
- Ultrashort pulses with a duration of 10 fs can work as driving field to generate attosecond pulses via high order harmonic generation.
- Ultrashort pulses can also be used in chemistry in order to obtain time-resolved visualization of molecular dynamics, which can be very fast reactions.
- Short pulses can also be used to engrave very small words/product names in metals and glasses without trashing the boundaries. However, pulse durations in the femtosecond order of magnitude are not required, durations in the picosecond region are sufficient.

5.1 Conclusions

The shortest pulse duration obtained with this post-compression technique is $\tau_{FWHM} \approx$ **10 fs** with a **50 μJ output energy**. However, the average pulse duration measured on a day-to-day basis is approximately 14 fs. This means that the compression factor, S, is 2 – 3 since the original pulse duration before compression is 30 fs.

The experiments in this Master Thesis are very similar to the ones done in [1] and [3], which has also been of great help during the preparations of the lab work. The compression factors are in those cases greater, but pulses produced here are in the 10-15 fs region compared to the other authors' values of 20-30 fs. The work on this experiment will be continued and the compression factor might increase, resulting in even shorter pulse durations.

It is very interesting to look at non-linear behaviour in common glass materials since this research area has not been included in my courses at LTH. During the lab work I have learnt a lot about working with lasers and especially the importance to properly check the alignment of the beam. Some minor mistakes have been made during the preparations, such as errors in the calculations of the bulk thickness, and the writing of the report have shown me that the theoretical background includes a lot of details and is quite complex. It has been great fun and all the practical details during lab work, too many to mention here, have given me a picture of the daily life at a laser research lab.

5.2 Outlooks

In this Master Thesis, a solid glass material (BK-7) is used to create pulse compression at the terawatt laser facility at CELIA, Bordeaux Université-1. The solid material broadens the pulse depending on SPM and GVD, which give the pulse a linear chirp that is removed by the prism compressor resulting in shorter pulse duration than the incoming pulse.

There are several improvements of the system that can be done such as optimising the length of the bulk to the set-up of the beam. Also more dispersive materials could be tried in order to get a bigger broadening and increased compression factor as a result.

One problem with the experiment is the use of a pinhole that effectively reduces the transmitted energy. It is noticed in this Master Thesis that a pinhole as big as 400 μm does not affect the short pulse duration and perhaps this might be the case for an even bigger pinhole and the advantage would then be an increase of the energy transmission.

The pulses are measured with a multi shot autocorrelator, but perhaps a single shot autocorrelator would be more advantageous.

Another idea is to couple the beam after the bulk directly into a hollow fiber. The beam will then be more homogenous and as a consequence more stable to work with. Experimental improvements performed after the end of my work were to install a spatial filter before the compressor and move the pinhole to the beam waist (focus). The beam is stable and 12-15 fs pulses with an output energy of 200 μJ are produced. The experiments also give the same results no matter if a multishot or a single shot autocorrelator is used.

6 Acknowledgements

I would like to thank the following people

- My two supervisors ***Eric Constant*** and ***Erik Mevel*** for all their help and support during my work at CELIA, Université Bordeaux 1.

- The head of department, ***François Salin***, for accepting me to CELIA, Université Bordeaux 1.

- ***Anne L'Huillier*** at the Division of Atomic Physics at LTH, Lund University for arranging the possibility for me to go to Bordeaux. I also want to thank her for being my supervisor at LTH and for giving me a lot of corrections and helpful comments on my report. Also I do much appreciate her patience during the extra time it took for me to correct the report.

- ***Tomas Christiansson*** formerly at the Division of Atomic Physics at LTH, now at GasOptics Sweden AB (Ideon, Lund) for being so supportive, reading through the report so many times and giving suggestions on improvements. The discussions we've had have been very helpful ☺

7 References

[1] C. Rolland and P. B. Corkum. Compression of high-power optical pulses. *J. Opt. Soc. Am. B*, Vol 5:641-647, 1988.

[2] S. A. Diddams, H. K. Eaton, A. A. Zozulya and T. S. Clement. Characterizing the non-linear propagation of femtosecond pulses in bulk media. *IEEE J. Selected topics in Quantum Electron.*, 4(2):306-315, 1998.

[3] V. Petrov, W. Rudolph and B. Wilhelmi. Compression of high-energy femtosecond light pulses by self-phase modulation in bulk media. *J. Mod. Opt*, 36(5):587-595, 1989.

[4] A. E. Siegman. *Lasers*. University Science books, 1986.

[5] J. Mauritsson. Generation of ultrashort laser pulses using gas-filled hollow waveguides, Master Thesis. *Lund Reports on Atomic Physics*, LRAP-247, 1999.

[6] Robert W. Boyd. *Nonlinear Optics*. Academic Press, 1992.

[7] O. Svelto. *Principles of lasers*. Plenum, 1998.

[8] G. P. Agrawal. *Nonlinear fiber optics*. Academic Press, 1989.

[9] J-C Diels and W Rudolph. *Ultrashort laser pulse phenomena*. Academic Press, 1996.

[10] M Nisoli, S. De Silvestri and O. Svelto. Generation of high energy 10 fs pulses by a new pulse compression technique. *Appl. Phys. Lett.*, 68(20):2793-2795, 1996

[11] F. Dorchies, J. R. Marquès, B. Cros, G. Matthieussent, C. Courtois, T. Vélikoroussov, P. Audebert, J. P. Geindre, S. Rebibo, G. Hamoniaux and F. Amiranoff. Monomode guiding of 10^{16} W/cm^2 laser pulses over 100 Rayleigh lengths in hollow capillary dielectric tubes. *Phys. Rev. Lett.*, 82(23):4655-4658.

[12] E.A.J Marcatili and R.A. Schmeltzer. Hollow metallic dielectric waveguides for long distance optical transmission and lasers. *Bell Syst. Tech. J.*, pages 1783-1809, 1964.

[13] E. Hecht. *Optics*. Addison-Wesley Publishing Company, 1987.

[14] Melles Griot. *Melles Griot Catalog*. 1999.

[15] CVI laser corporation. Femtosecond laser mirrors. *CVI laser Optics*. p. 32-36.

[16] SHOTT. *Verre d'optique*. 1986.

[17] B. E. A. Saleh, Malvin Carl Teich. *Fundamentals of photonics*. John Wiley & sons, Inc, 1991.

8 Appendices

8.1 Gaussian Beams

A laser beam travelling along the z-axis can be described as a Gaussian beam. Gaussian beams are a class of solutions to the E-field in the Schrödinger equation and can be seen as a spherical of complex radius of curvature [7]

$$\overline{E}(x,y,z) \propto e^{-\left[\frac{x^2+y^2}{w^2}\right]} \cdot e^{-ik\left[z+\left(\frac{x^2+y^2}{2R}\right)\right]} \tag{33}$$

where w is the beam spot size for the electrical field at the position z and R is the waves radius of curvature. The beam spot size, w, is expressed with the Rayleigh length, z_R (explained below), as

$$w(z) = w_0\sqrt{1+\frac{z^2}{z_R^2}} \tag{34}$$

The beam spot size of the intensity profile, w_I, is defined as the value at which $I = I_{max}/e$. The area of a Gaussian beam is then

$$A = \pi\, w_I^2 = \pi\left(\frac{w}{\sqrt{2}}\right)^2 = \frac{\pi\, w^2}{2} \tag{35}$$

and since $I \propto E^2$ the intensity becomes

$$I = I_{\max} e^{-\left[\frac{2x^2+y^2}{w^2}\right]} = I_{\max} e^{-r^2/w^2} = \frac{2P}{\pi\, w^2} e^{-r^2/w^2} \tag{36}$$

I_{max} is in the equation substituted $I_{max} = P/A$ where P is the power of the Gaussian beam. At the focal point the Gaussian beam size, w_0, is called the *beam waist* and is not given by geometrical optics but by

$$w_0 = \frac{f\lambda}{\pi\, w} \tag{37}$$

where f is the focal length of the focusing material, λ is the wavelength, w is the beam size when the beam enters the focusing element. The length of the focus in the propagation direction along the z-axis can be of interest, especially when experimentally producing a laser system. The length of the focus is called the Rayleigh length

$$z_R = \frac{\pi\, w_0^2}{\lambda} \tag{38}$$

The Rayleigh length is defined as the distance from focus to where the beam diameter has increased by a factor $\sqrt{2}$. Now the Gaussian beam's radius of curvature is given by a simple expression

$$R(z) = z + \frac{z_R^2}{z} \tag{39}$$

where z is the distance from the focus.

8.2 *The Non-linear Schrödinger equation*

The main difference between pulse propagation in a mono-mode fiber and in a bulk material is that the fiber propagation problem can be reduced to only one space coordinate whereas the bulk case needs at least one additional spatial coordinate in order to get cylindrical symmetry. The second coordinate describes the change of intensity across the beam cross-section and the change of the beam diameter and beam profile along the way through the bulk. According to [2] the wave propagation through a bulk could be described with the one-dimensional non-linear Schrödinger equation (1-D NLSE), but then the combined effect of diffraction with normal dispersion and also cubic non-linearity will not be included. These effects can lead to *Self-Focusing* (*SF*) and pulse splitting effects that have to be avoided during these experiments.

The propagation of ultrashort pulses through a bulk with dispersion is given by the (3-D) non-linear Schrödinger wave equation (NLSE). The NLSE for bulk materials has been explored in [2] and in the case of radial dependence it is given by

$$\frac{\partial \overline{E}}{\partial z} + i\frac{\beta_2(\omega_0)}{2}\frac{\partial^2 \overline{E}}{\partial t^2} - i\frac{1}{2\beta(\omega_0)}\frac{\partial^2 \overline{E}}{\partial r^2} - i\frac{\beta(\omega_0)n_2}{n_0}\left|\overline{E}\right|^2 \overline{E} = 0 \qquad \text{NLSE} \tag{40}$$

where ω_0 is the laser's central frequency and $E(z, r, t)$ is the slowly varying complex amplitude of the electric field and the field is normalized so that $|E(z, r, t)|^2 = I$ is the intensity. The propagation direction through the material is denoted z and r gives the radial dependence. n_0 is calculated around the laser's central frequency and n_2 is the non-linear refractive index of the specific material.

As mentioned in the chapter *Group velocity dispersion (GVD*, 2.2, the first derivative of the propagation constant β (with respect to frequency) is the group velocity, $\beta_1 = v_g$ and the second derivative, β_2, corresponds to pulse broadening due to the GVD. The third propagation term corresponds to the radial variation of the pulse shape and hence the distribution of intensity while the fourth term is the broadening due to SPM.

Discussion of, and solutions to the NLSE are found par example in references [2] and [3]. A very good step by step derivation of the NLSE for a capillary as well as the expressions for the higher order effects such as self steepening and third order dispersion (TOD) are found in [5].

8.3 *Autocorrelators*

For ultrashort laser pulses there is no electronic machine that can measure the pulse duration. Non-linear optics has to be used to measure this kind of short pulses. Up until today the most used method is to use a second harmonic autocorrelator technique. The autocorrelator makes use of the fact that even if the laser pulses are very short, they travel with the speed of light a distance corresponding to the pulse duration. With a pulse duration of approximately 10 fs (which is slightly shorter than in this Master Thesis) the distance travelled will be around 3 μm. So, the pulse is measured even if it is not possible to measure it directly.

The idea of the multi shot autocorrelator is discussed below and this is the kind of autocorrelator that was used in the experiments. In the case of very fluctuating pulses or a slow repetition rate, a single shot autocorrelator would be more convenient. The single shot autocorrelator is basically the same as a multi shot but it is enough with a single pulse to make the measurement.

8.3.1 Multi shot autocorrelators

A multishot correlator is depicted in the big Figure 15 on the next page and it might be useful to watch the picture while reading the following explanation of how it is working. The laser beam enters the autocorrelator where it is divided into two pulses by a beam splitter mirror. The two pulses now passes two different delay lines of which one is controlled by a variable translation stage (micrometer screw on one side of the autocorrelator) while the other one is fixed from the beginning but can be moved by a stepper motor. The delay line with the stepper motor is tuned to have zero difference to the other delay line exactly half way between the end points.

Both pulses are combined in a frequency doubling crystal made of either BBO or KDP, which are both birefringent materials. If the birefringent crystal is correctly oriented for phase matching conditions second harmonic light with the frequency 2ω will be generated in the direction of the two pulses propagation direction. Now, if the two pulses overlap both temporally and spatially a bisector with second harmonic light will be created between the two pulses. The frequency doubled light in the bisector is the autocorrelator signal and it is measured with a slow integrating photo detector.

The signal is proportional to the *intensity autocorrelation function* given by [5]

$$S(\tau) \propto \int_{-\infty}^{\infty} I(t)I(t-\tau)dt \tag{41}$$

When the stepper motor moves one of the delay lines the value of τ changes at the same time as the signal is measured. The time duration of the laser pulses is then calculated by using $S(\tau)$. The FWHM of the autocorrelation function is called the autocorrelation trace, denoted τ_{ac}, and is proportional to the FWHM of the pulses time duration, τ_p,

$$\tau_p = \frac{\tau_{ac}}{a} \tag{42}$$

Since the pulse is assumed to have a $sech^2$ shape the constant is $a \approx 1{,}543$. However, if the pulse is thought to be of Gaussian shape the constant is $a \approx 1{,}414$. The signals from the autocorrelator are shown at an oscilloscope screen where one channel corresponds to the autocorrelation trace and the other corresponds to the moving arm. The FWHM is measured on the screen and then recalculated to the real pulse duration.

The multi shot autocorrelator uses several pulses to create the autocorrelation trace and this suggests that the pulses must be approximately regular and have the same appearance on a shot to shot basis. If the laser is fluctuating a lot that makes the multi shot autocorrelator difficult to use and the results a bit unreliable. In that case a single shot autocorrelator might be of better assistance.

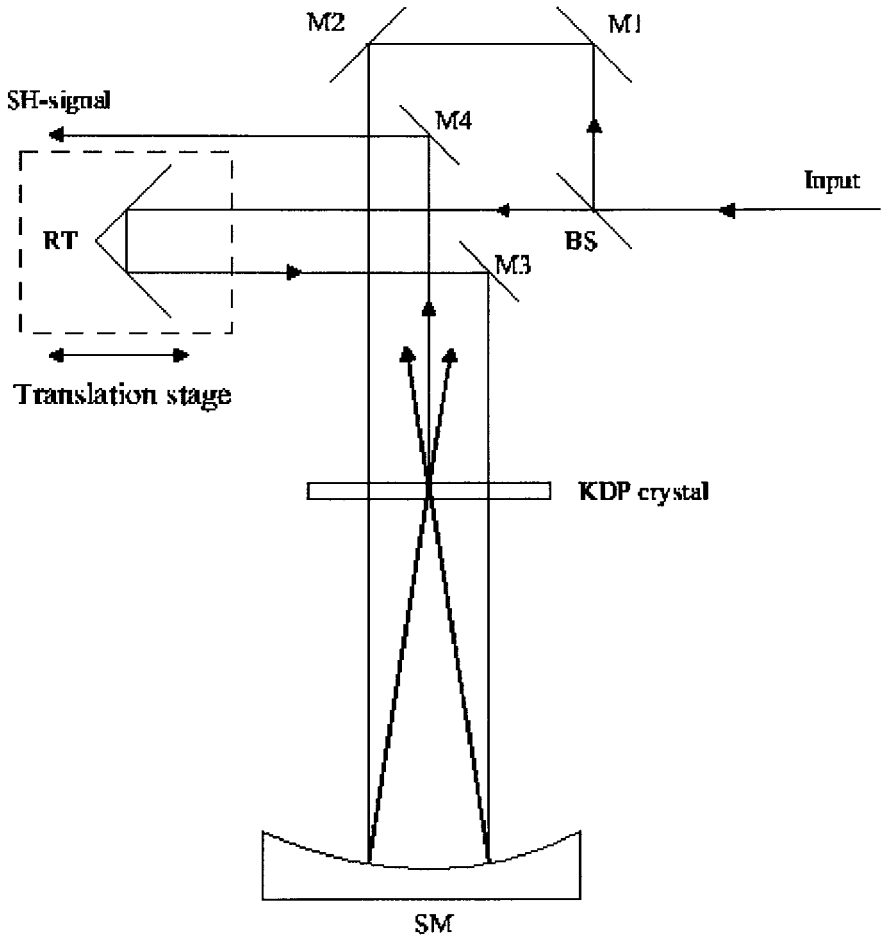

Figure 15. The design of a multishot autocorrelator (Figure 29 from [5]). The input beam is split into two parts by the beam splitter (BS). One of the pulses passes a variable delay line controlled by a translation stage (micrometer screw on the side of the autocorrelator) while the other passes delay line wich is controlled by a stepper motor. Mirror M1-M4 are guiding mirrors and RT is a roof top mirror. The beams are focused into a birefringent crystal and at correct phase matching conditions a second harmonic signal is created at the bisector of the two beams if they overlap both spatially as well as temporally.